Talanta 116 (2013) 26–32

Contents lists available at ScienceDirect

Talanta

journal homepage: www.elsevier.com/locate/talanta

On-chip electrochemical microsystems for measurements of copper and conductivity in artificial seawater

Grégoire Herzog *,[1], Waleed Moujahid, Karen Twomey, Conor Lyons, Vladimir I. Ogurtsov **

Tyndall National Institute, University College Cork, Lee Maltings, Cork, Ireland

ARTICLE INFO

Article history:
Received 26 November 2012
Received in revised form
17 April 2013
Accepted 24 April 2013
Available online 4 May 2013

Keywords:
Microfabrication
Underpotential deposition-stripping voltammetry
Impedance
Environmental parameters

ABSTRACT

The fabrication and characterisation of microelectrochemical sensors for Cu^{2+} and conductivity suitable for operation in the marine environment are presented. The impact of the designs on sensor performance and their adequacy to operate in real conditions are discussed. The sensors, tailored to voltammetric and impedimetric measurements, are fabricated on silicon using photolithographic and thin film deposition techniques. The impedimetric sensor is made of Pt interdigitated electrodes which are used for the measurement of conductivity. The voltammetric sensors are based on a three electrode electrochemical cell with on-chip Ag|AgCl reference and Pt counter and working electrodes, used for detection of copper by underpotential deposition-stripping voltammetry at microelectrode array. The sensors operated in the Cu^{2+} concentrations ranging from 0.48 to 3.97 μM with a limit of detection of 0.115 μM. The impact of the temperature, the pH and the salinity of the artificial seawater on the sensitivity for Cu^{2+} detection are also considered. Measurements of copper concentration and conductivity are validated using certified reference materials and standard solutions.

1. Introduction

Electrochemical methods are of particular interest for in-situ environmental applications as operating procedures remain simple and are without or with limited sample pre-treatment, which is essential for their implementation outside the laboratory. Miniaturised electrochemical sensors offer a number of advantages over macroscopic electrodes including (i) improved mass transport and hence increased sensitivity (due to the hemispherical diffusion); (ii) improved signal to noise ratio; (iii) reduced *iR* drop [1]. Thus, microfabricated electrochemical sensors can provide sufficient sensitivity and achieve required limits of detection for practical applications due to improved mass transfer and signal to noise ratio. A number of miniaturised electrochemical sensors for autonomous in-situ measurements have been developed [2–9]. Autonomous electrochemical systems were devoted to the detection of heavy metals in sea water by either cathodic stripping voltammetry [2,3] (CSV) or anodic stripping voltammetry [4–7] (ASV). Concentration of dissolved oxygen in seawater has also been monitored using electrochemical sensors [8,9]. These types of sensors have been incorporated within autonomous monitoring systems for in-situ measurements [10]. More recently, wearable electrochemical sensors and instrumentation have been integrated into a watersport wetsuit [11]. Three types of amperometric sensors (for phenol, heavy metals and trace explosive) were incorporated in the garment. Chemical and physical sensors can be integrated in autonomous environmental monitoring systems, which allow the measurements of pollution and quality levels in fixed sampling locations [11–17].

In our previous studies, we have investigated the impact of the microelectrode array design on the cyclic voltammetry response of ferrocene monocarboxylic acid [18]. Such microelectrode arrays have also been modified with conducting polymers or thiols for the detection of hydrogenophosphate in organic solvents [19]. More recently, reference and counter electrodes were integrated into a single chip and characterised in artificial sea water by cyclic voltammetry of ferricyanide [20]. We report here the use of microfabricated electrochemical sensors for the measurement of Cu^{2+} concentration and conductivity in artificial seawater. Cu^{2+} has been selected as a model pollutant present in seawater. Cu^{2+} can be found at relatively high concentrations in port and marina waters due to the leaching, in such a confined space, of Cu^{2+} from antifouling paints on vessels [21,22]. Conductivity is related to seawater salinity, which has an impact on sensitivity for Cu^{2+} detection. Conductivity measurement could be used to correct the Cu^{2+} concentration measured. It can also indirectly indicate the presence of pollution. Cu^{2+} is detected by

---

* Corresponding author. Present address: Université de Lorraine, LCPME, UMR 7564, Villers-lès-Nancy F-54600, France. Tel.: +33 3 83 68 52 54.

** Corresponding author. Tel: +353 21 490 4271.

E-mail addresses: gregoire.herzog@univ-lorraine.fr (G. Herzog), vladimir.ogurtsov@tyndall.ie (V.I. Ogurtsov).

[1] Present address: CNRS, LCPME, UMR 7564, Villers-lès-Nancy F-54600, France.

0039-9140/$ - see front matter © 2013 Elsevier B.V. All rights reserved.
http://dx.doi.org/10.1016/j.talanta.2013.04.057

underpotential deposition-stripping voltammetry (UPD-SV) as it offers a number of advantages for electroanalytical applications [23]. Underpotential deposits only cover a small portion of the electrode surface, leaving the electrode surface mainly unchanged. At the maximum, only a monolayer is deposited so the preconcentration times are short; finally, this method allows detection of metals in the presence of dissolved oxygen. Furthermore, the suggested approach does not require a special sample preparation protocol which calls for complex fluidic systems. This circumstance coupled with the employment of microfabricated sensors makes this detection technique very attractive for on-board autonomous monitoring applications where the requirements on robustness, low size and power of the sensing system are essential.

The microelectrochemical system was implemented with two types of sensors fabricated using photolithographic techniques. The first type of sensor was a three-electrode cell made of a platinum working microelectrode array, a Ag|AgCl reference electrode and a platinum counter electrode. The second type was made of platinum interdigitated electrodes. The three-electrode cell was characterised by cyclic voltammetry of ferricyanide in artificial seawater and was subsequently used for UPD-SV of Cu^{2+}. In the literature, the performance of miniaturised electrochemical sensors, and of microelectrode arrays are mostly evaluated and discussed based on cyclic voltammetry experiments [24,25]. However, this electrochemical method is seldom used for analytical applications due to its lack of sensitivity. Indeed, stripping voltammetry techniques at micro-electrode arrays are generally used for the detection of metals in solution [26]. The influence of the geometry of the microelectrode array (radius, spacing, number of electrodes) on the analytical response of Cu^{2+} UPD-SV is discussed in order to optimise the microelectrode array design to achieve the best analytical performance. Conductivity of artificial seawater was measured by application of electrochemical impedance spectroscopy at the interdigitated electrodes of different designs.

2. Experimental

2.1. Microfabrication and microelectrochemical cell design

The sensors designed for this work were: a three-electrode cell for voltammetric detection and an interdigitated electrode pair for impedimetric measurements. The sensors were fabricated as described previously on individual chips [18–20].

The three-electrode Pt cell comprised a working microelectrode array, an L-shaped counter electrode and a pad for the reference electrode was fabricated at the first stage of the process (mentioned above). To prepare the reference electrode, a drop of silver paint was placed on the Pt pad, and the silver paint was cured at 120 °C for 1 h. The silver paint is then oxidised by cyclic voltammetry in 1 M KCl between 0 and 1 V at scan rate 10 mV s^{-1} to form a Ag|AgCl electrode. Eight working microdisc electrode arrays (named A1 to A8) in a hexagonal arrangement were designed with different numbers of electrodes in the array (N=4, 16, 64 or 256), different electrode radii (r=5, 10, 15 and 20 μm) and different inter-electrode spacing (S=200 and 400 μm). Four designs of interdigitated electrodes (named I1 to I4) for conductivity measurements were fabricated with varying geometrical parameters: electrode length, width and spacing. The geometric parameters of these designs are summarised in Table 1. Each fabricated chip was made of one electrochemical cell or one set of interdigitated electrodes.

2.2. Electrochemical measurements and reagents

All electrochemical experiments were performed in a Faraday cage and each measurement was carried out four times (unless stated otherwise). The sensors were cleaned beforehand in a plasma cleaner (Harrick Plasma, New-York, USA) for 5 min at high frequency at 100 W, 600 m Torr. A CHI620A potentiostat of CH Instruments (purchased from IJ Cambria, Burry Port, Wales, UK),

Table 1
Geometrical parameters of the different microchemical cells designed (A1-A8 & I1-I4).

Design	r/mm	d	N	A_{CE}/cm^2	Geometry
Microelectrochemical cells					
A1	10	20r	4	0.030	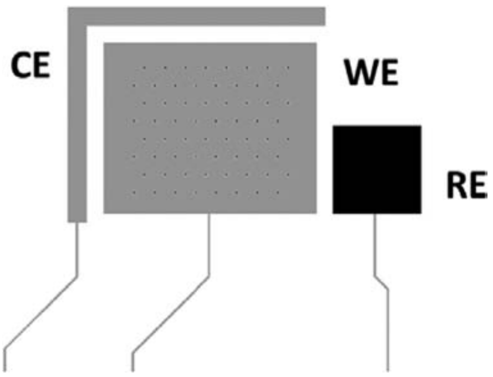
A2	10	20r	16	0.030	
A3	10	20r	64	0.075	
A4	10	20r	256	0.300	
A5	5	20r	64	0.030	
A6	15	20r	64	0.075	
A7	20	20r	64	0.180	
A8	10	40r	64	0.180	

Design	w/mm	L/mm	d/mm	N	Geometry
Interdigitated electrodes					
I1	20	3500	10	63	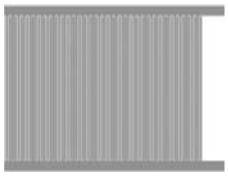
I2	40	3500	10	40	
I3	20	1500	10	63	
I4	20	1500	40	40	

r: radius of the microdisc, d: interelectrode distance; N: Number of elements in the array; ACE: Surface area of the counter electrode; CE: Counter electrode; WE: Working electrode; RE: Reference electrode; w: width; L: length.

linked to a personal computer, was used for the voltammetric studies. The stripping of the copper underpotential deposits was done by SW voltammetry with the following parameters: amplitude: 25 mV; frequency: 15 Hz, increment: 4 mV. Impedimetric measurements were performed by electrochemical impedance spectroscopy (EIS) using an Autolab PGSTAT302N electrochemical workstation from Metrohm Ltd. The temperature of the tested solutions was set at 25 °C using a LaudaEcoline Model E-200 circulator. EIS was performed over the frequency range 0.1 Hz–1 MHz at an applied potential of 0.2 V DC bias and a 5 mV AC amplitude.

All chemicals used in this study were purchased from Sigma-Aldrich Ireland Ltd. and used as received. The electrolyte solution employed in the experiments was artificial seawater with the following composition: 400 mMNaCl, 20 mM $MgCl_2$, 20 mM $MgSO_4$, 10 mM $CaCl_2$ and 10 mMKCl [27,28]. The pH of the solution was adjusted to 6.5 by addition of HCl. Control of pH was performed using a Benchop pH/ISE meter Model 520A (Orion Research Inc. USA) which was calibrated before each use. Artificial seawater of varied salinity was prepared according to ratios published by Hansson [29]. The reference material “LGC6016 Estuarine water-Traces metals” used for the Cu sensor validation was purchased from LGC Standards (UK) and represented estuarine water taken from the Seven Estuary, UK, offshore from a heavily industrialised area near Avonmouth. The conductivity sensors were characterised over a range of standard KCl solutions with conductivity values equal to 1.413, 10.00, 12.90, 20.00 and 50.00 mS cm^{-1} within which the range of seawater conductivity coincides. The conductivity standards were purchased from Sigma Aldrich and Reagecon Ltd. A standard conductometer (712 Conductometer from Metrohm, Switzerland) was used to measure the conductivity of artificial seawater and standard KCl solutions.

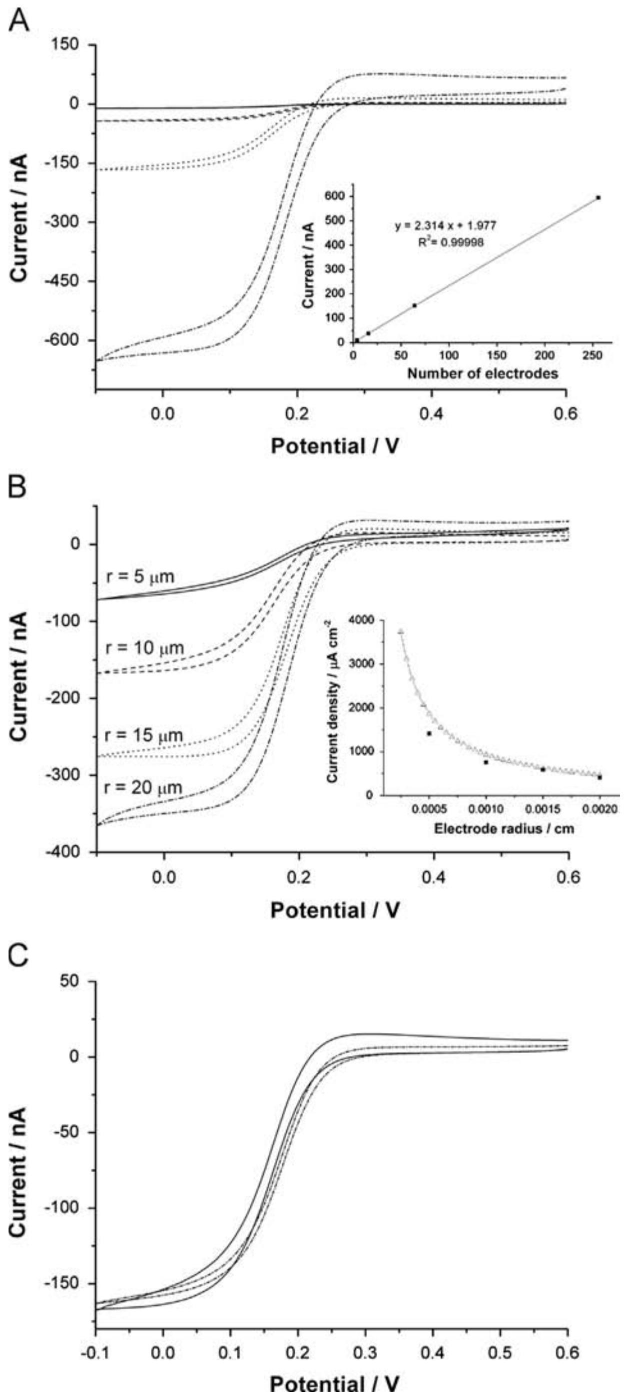

Fig. 1. Cyclic voltammetry of 1 mM ferricyanide in artificial seawater using microelectrochemical cells of (A) designs A1–4 (voltammograms from top to bottom). Inset: i_{lim} as a function of N; (B) designs A3, A5–7. Inset: limiting current density as a function of r; (C) designs A3 and A8. The scan rate was 10 mV s^{-1}.

3. Results and discussion

3.1. Characterisation of the microelectrochemical cell

The fabricated microelectrochemical cells were tested by cyclic voltammetry of 1 mM ferricyanide in artificial seawater at scan rate 10 mVs^{-1} (Fig. 1). In all cases, a sigmoidal shape was observed for each of the designs A, indicating an occurrence of hemispherical diffusion of the ferricyanide towards the microdiscs with absence of overlapping between the diffusion zones of neighbouring microdiscs for the timescale of the experiments. The limiting currents, i_L, obtained experimentally for the different designs by averaging of 6 experiments were then compared to the theoretical values calculated from Eq. (1) [30]:

$$i_L = \frac{4\pi nFDCr^2N}{4L + \pi r} \tag{1}$$

Here, n is the number of electron exchanged in the reaction ($n=1$), F is the Faraday constant (96,485 C mol^{-1}), D is the ferricyanide diffusion coefficient ($D=7.6 \times 10^{-6}$ cm^2 s^{-1} [31]), C is the bulk concentration (in mol cm^{-3}), r is the radius of the microdisc (in cm), N is the number of microdiscs in the array and L is the recess due to the silicon nitride layer (5×10^{-5} cm). The equation implies that the microdiscs in the array are sufficiently spaced in such a way that there is no overlap of the diffusion zones of neighbouring electrodes. The experimental and theoretical values of the limiting current were similar, that confirmed the adequate spacing and the suitable fabrication process. Fig. 1A shows the voltammograms for designs A1–A4 with the number of microdiscs in the array varied from 4 to 256. The radius (r) and spacing (S) were kept constant ($r=10$ µm and $S=200$ µm). The limiting currents increased linearly with the number of microdiscs in the array (inset of Fig. 1A) with a slope of 2.3 nA per electrode with a coefficient of determination $r^2=0.99998$. The experimental values of the limiting currents (in round brackets) in comparison with the theoretical ones obtained by using Eq. (1) [in square brackets] were as follows: (10.4 ± 0.19) nA vs. [11.0 nA] for design A1, (38.6 ± 2.02) nA vs. [44.1 nA] for design A2, (152 ± 3.84) nA vs. [176 nA] for design A3 and (594 ± 4.87) nA [706 nA] for design A4. As one can see the theoretical limiting current exceeded the experimental data providing a discrepancy between current values in the range between 6% and 18%. The discrepancy as the number of microdiscs in the array increased, which can be attributed to the presence of 'dead' or inactive μdiscs in the array, which eventually lead to a lower limiting current [32,33].

Fig. 1B shows the voltammograms for designs A3, A5, A6 and A7, with the radius r varied from 5 to 20 μm. The number of microdiscs in the array N was equal to 64, and the centre-to-centre spacing S was kept equal to $20r$. The limiting current values increased with increasing electrode radius as expected from Eq. (1). However, the current density increased when the radius decreased (see inset in Fig. 1B) due to the improved mass transport at microdiscs of smaller dimension. Once again, the experimental limiting current values were in reasonable agreement with the theoretical values: (71.1 ± 5.61) nA vs. [83.3 nA] for design A5, (152 ± 3.84) nA vs. [176 nA] for design A3, (267 ± 2.86) nA vs. [270 nA] for design A6 and (334 ± 3.99) nA vs. [364 nA] for design A7 (discrepancy between current values was between 8% and 17%). Once more, the theoretical limiting current exceeded the experimental data. Again this discrepancy can be attributed to the presence of inactive electrodes in the array.

The influence of centre-to-centre spacing between neighbouring microdiscs on the limiting current is shown in Fig. 1C by example of the array with $r = 10$ μm. The neighbouring microdiscs spacing S was $20r$ (design A3) and $40r$ (design A8). No significant differences between the experimental limiting currents were observed: (152 ± 3.84) nA for design A3 and (146 ± 4.83) nA for design A8.

3.2. UPD-SV of Cu^{2+}

As preliminary experiments, a series of three UPD-SV scans was performed: (1) UPD-SV in artificial seawater in the absence of copper; (2) a UPD-SV of 1.5 μM Cu^{2+} in artificial seawater and (3) UPD-SV in artificial seawater in the absence of copper. After the third scan, a residual underpotential deposit of Cu was stripped from the surface of the electrode (data not shown). This indicated the need to introduce electrochemical steps to produce a fresh and clean electrode surface for the subsequent measurements. The potential waveform for the UPD-SV procedure was the following [34]: (1) a preconditioning step at+0.8 V for 5 s; (2) a cleaning step at+0.45 V for 45 s; (3) a preconcentration step at −0.15 V for 90 s; (4) a detection step by square wave voltammetry starting at −0.15 V and finishing at 0.6 V (Fig. 2A). The preconditioning and the cleaning steps are necessary to remove any residual metal underpotentially deposited during previous experiments. The application of this procedure regenerated the sensor surface and produced a consistent reference CV prior to copper detection (data not shown). The 90 s preconcentration time was selected based on previous work on the UPD-SV of copper at microelectrode arrays [20].

UPD-SV of copper at the eight different microelectrochemical cells was then undertaken for increasing concentrations of copper using the procedure described above. Fig. 2B shows the UPD-SV results for design A4 for concentrations ranging from 1 to 5 μM. A calibration curve for copper is shown in inset. For each concentration, the stripping peak current value was the average of 6 measurements. Table 2 displays different sensor parameters for designs A1–A8. The sensitivity of UPD-SV depends on the diffusion type (hemispherical or linear) occurring at the microelectrodes during the preconcentration step. The diffusion type is itself related to the geometrical parameters of the microelectrochemical cells. As expected, the geometrical parameters of the microelectrode array had a strong influence on it as it varied from 0.38 nA μM^{-1} for design A1 up to 13.59 nA μM^{-1} for design A7. Good linearity between the stripping peak currents and the concentration was achieved for the designs studied. The influence of the geometry of the array (number and radius of the microdiscs and inter-electrode spacing) on the sensitivity was investigated. The sensitivity was normalised to the surface area of the microdiscs in the array for comparison purposes. The normalised sensitivity as a function of the number of microdiscs in the array is shown in Fig. 3A. It can be expected that the normalised sensitivity should be constant in the case of microdiscs demonstrating independent diffusion behaviour. Nevertheless from Fig. 3A, it clearly appears that the normalised sensitivity varies with the number of microdiscs in the array. Such results suggest that microdiscs do not behave independently from one another and overlap of the diffusion zones occurs. Deviation from the constant value is observed at the two arrays with the larger number of microdiscs. This can be explained by the fact that in an array, the nature of the microdiscs can be divided in two types: peripheral and central microdiscs, as illustrated in inset of Fig. 3A for an array of 16 microdiscs. Central microdiscs have 6 neighbours and are more likely to suffer from overlap of the diffusion zones and hence their contribution to the total current reduces drastically. The proportion of central microdiscs in the array increases with the number of discs in the array. For design A1 ($N = 4$), there are no central microdiscs, whereas 56% of discs in design A3 ($N = 64$) and 76% of discs in design A4 ($N = 256$) are central microdiscs. This overlap between the diffusion zones is observed for the Cu UPD-SV experiments although CV experiments shown in Fig. 1A demonstrated independent microdiscs. This was due to the difference between the timescale of the cyclic voltammetry of ferricyanide and the UPD-SV experiments for Cu^{2+} detection. Indeed, the distance between neighbouring microdiscs in an array

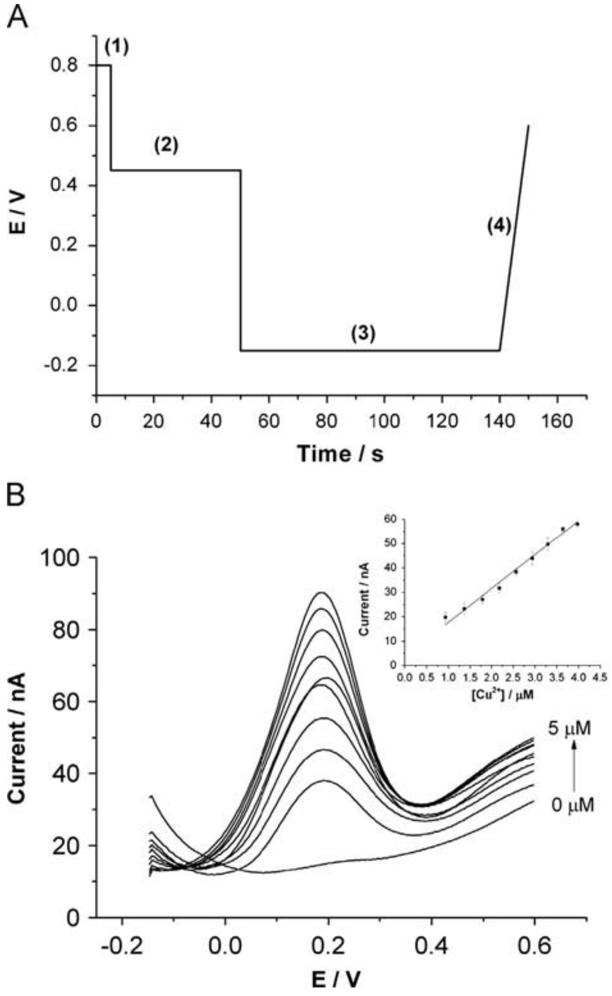

Fig. 2. (A) Potential waveform for the Cu^{2+} UPD-SV experiments at the different microelectrochemical cell designs, (B) UPD-SV of Cu^{2+} ($0 < [Cu^{2+}] < 5$ μM). Inset: calibration curve of the Cu^{2+} stripping current as a function of the Cu^{2+} concentration in artificial seawater.

Table 2
Analytical performances for the Cu^{2+} UPD-SV at the different microelectrochemical cells designed (A1–A8).

Design	Dynamic Range (mM)	Sensitivity (nA mM^{-1})	Sensitivity (μA mM^{-1} cm^{-2})	Intercept (nA)	R^2	LOD (mM)
A1	0.48–3.97	0.38	30.2	0.18	0.990	0.34
A2	0.48–2.94	1.92	38.2	1.35	0.998	0.11
A3	0.93–3.97	5.12	25.4	2.30	0.994	0.24
A4	0.93–3.97	13.49	16.8	4.69	0.986	0.39
A5	0.48–2.94	2.05	40.8	2.70	0.988	0.30
A6	0.59–2.91	5.42	23.5	11.70	0.988	0.28
A7	0.48–2.94	13.59	16.9	5.90	0.996	0.13
A8	0.48–2.94	7.87	39.1	6.32	0.992	0.23

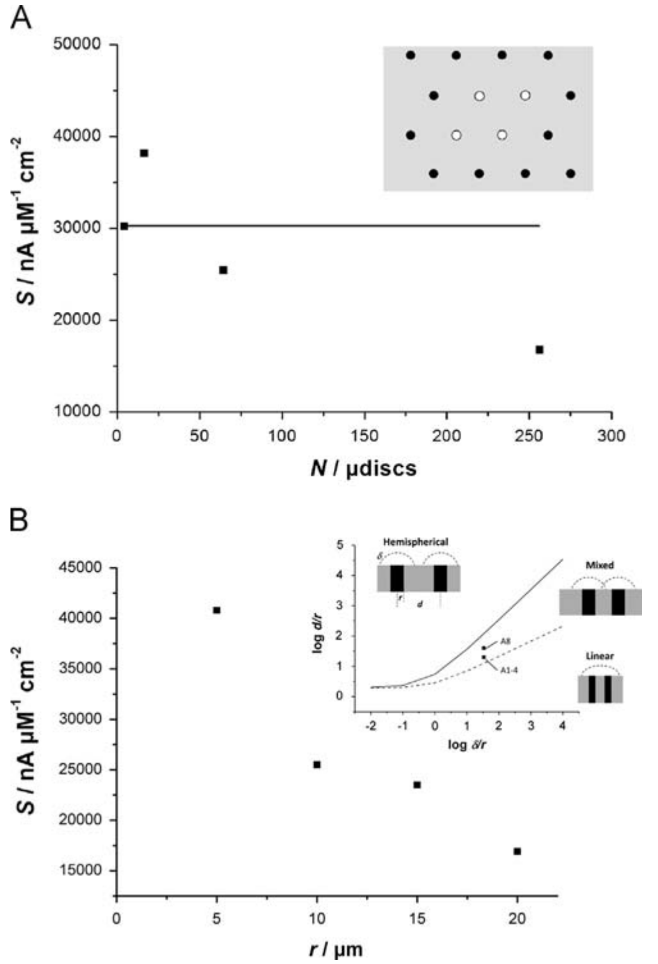

Fig. 3. (A) Sensitivity normalised to the surface area as a function of microdiscs in the array (▴). The straight line represents the expected behaviour if microdiscs in the array were independent from one another. Inset: schematic representation of the array (design A2) where (•) are the peripheral microdiscs and (○) are the central microdiscs, (B) sensitivity normalised to the surface area as a function of microdisc radius. Inset: plot of log d/r vs. lod δ/r for electrodes of designs A1–A4 and A8. The solid line is described by Eq. (3) and the dotted line by Eq. (4) [36].

needed to be 20r to ensure hemispherical diffusion (according to the empirical rule) was valid for short timescales such as cyclic voltammetric experiments. However, in the case of UPD-SV at the end of the preconcentration step of 90 s, the diffusion layer corresponded to 357 μm thickness as follows from Eq. (2) [30]:

$$\delta = \sqrt{2Dt} \tag{2}$$

In this equation, δ is diffusion layer thickness, D is the diffusion coefficient of copper ions ($D = 7.1 \times 10^{-6}$ cm^2 s^{-}) [35] and t is the preconcentration time. This is in agreement with previous studies by Menshykau et al. on the concept of diffusional independence [25]. Sensitivity normalised to the surface area increases when the microdiscs radius decreases as is shown in Fig. 3B. The sensitivity values range from 16.9 μA $μM^{-1}$ cm^{-2} (design A7, $r = 20$ μm) up to 40.8 μA $μM^{-1}$ cm^{-2} (design A5, $r = 5$ μm). This behaviour of the sensitivity as a function of the radius is expected and was also reported elsewhere [18]. Furthermore, when the inter-electrode spacing is increased from 20 times of the radius (design A3, $d = 200$ μm) to 40 times (design A8, $d = 400$ μm), the sensitivity rises from 25.5 to 39.1 μA $μM^{-1}$ cm^{-2}. These results confirm that overlap of the diffusion zones occurs during the deposition step of the UPD-SV experiments, although such an overlap was not observed for the CV experiments. Lee et al. have described diffusion at microdiscs arrays using two dimensionless parameters which are d/r and δ/r [36]. The plot of log (d/r) vs. log (δ/r) can be divided in three domains where diffusion is either spherical, linear or mixed (inset of Fig. 3B). These three domains are based on two equations as described by Lee et al. [36]. The limit between the hemispherical and the mixed diffusion domains is described by Eq. (3) and the limit between the mixed and the linear diffusion domains is described by Eq. (4).

$$\frac{\delta}{r} = \left[\frac{d}{2r} - 1\right] / \sqrt{3} \tag{3}$$

$$\frac{\delta}{r} = \sqrt{\frac{2}{\pi}}\left[\frac{\sqrt{3}d^2}{2\pi r^2} - 1\right] \tag{4}$$

Based on the geometrical parameters of the designs tested and the preconcentration time used for the experiments reported in this article, mixed diffusion processes are obtained and correlates with the results observed. In order to achieve fully hemispherical diffusion at a microdisc array, it is necessary to either shorten δ by reducing the deposition time or by increasing the inter-electrode spacing, d, or by a modification of both.

Limits of detection were calculated based on the y-intercept and slope values of the calibration curves constructed plus three times the standard deviation of the y-intercept values [37]. They ranged from 0.11 μM to 0.39 μM. There was no particular trend between the limits of detection achieved and the geometrical parameters of the electrode (number of microdiscs in the array, microdisc radius, inter-microdisc distance). This may have been due to the strong presence of chloride ions in seawater, which upon adsorption on the platinum surface were capable of interfering with the copper detection [38] as the chloride anions competed with Cu atoms underpotentially deposited on the surface. The competition between chloride ions and Cu was stronger than between sulphate ions and Cu. Therefore, the high concentration of chloride in seawater hindered the UPD of low concentration of Cu^{2+}. Nevertheless, the limits of detection achieved here are in the same order of magnitude as the Cu^{2+} concentrations that can be found in polluted port and marina waters [21,22]. Furthermore, the reference material analysed had a Cu^{2+} concentration of (2.96 ± 0.02) μM. The reference material was analysed by the standard addition method. UPD-SV scans on the sample were performed at design A6 microelectrochemical cell. Two standard additions of 3 μM of Cu^{2+} were added to the sample. Experiments were done in quadruplets. The standard addition linear regression was $y = 1.42x + 3.44$ ($r^2 = 0.970$) and the concentration extracted with this equation was (2.43 ± 0.50) μM which coincided, within the accuracy of the analysis, with the known copper concentration in the sample provided. The relatively large difference between the certified Cu^{2+} concentration and the measured one could be due to the presence of dissolved organic matter. The reference material was used as received. As no sample preparation was used, the presence of dissolved organic matter might foul the electrode surface and hence limits the sensitivity of the μdisc surface.

Previous studies have shown that Cu^{2+} UPD-SV can be inhibited by the presence of dissolved organic matter such as surfactants and humic acid [39–41]. This could be avoided by the use of a permselective gel membrane [42] or by the disorganised monolayer approach [39].

The influence of parameters such as the temperature, the pH and the salinity of the artificial seawater on the sensitivity for Cu^{2+} UPD-SV for different preconcentration times (PT) of 0, 45 and 90 s was also investigated (Fig. 4). A wide range of environmental conditions (pH, T and salinity) were selected to allow the study of behaviour of the microelectrochemical sensors in various conditions that may be encountered in the field. In the Atlantic Ocean, seawater temperatures can vary between 283 and 303 K during the year; and pH values have been measured between 6.5 and 8.5. Salinity is defined as the salt concentration in seawater. It is measured in practical salinity units (PSU). Salinity of seawater is measured by its conductivity. The average salinity of ocean water is 35.5 PSU, varying from less than 15 PSU at river mouths to more than 40 PSU in the Dead Sea [43]. Calibration curves for Cu^{2+} at microdisc array of design A6 were built for temperatures ranging from 283 to 303 K (pH was kept constant at 6.5, salinity was 30 PSU), for pH values between 6.5 and 8.5 ($T=298$ K, salinity=30 PSU) and for salinity values between 20 and 40 PSU (pH 6.5 and $T=298$ K). Fig. 4A shows that the sensitivity increases linearly with the T range under investigation as it was observed by Jerkiewicz et al. for the Cu^{2+} UPD studies in acidic solutions at Pt (111) electrodes [44]. For pH values between 6.5 and 8.5, the maximum sensitivity was obtained for pH 7.5 and the lower sensitivity was obtained for pH 8.5 (Fig. 4B), due to the increase of hydroxide ions in the artificial seawater solution. At diluted Cu^{2+} concentrations ($<10^{-5}$ M) and at pH between 6.3 and 8.5, free Cu^{2+} concentration decreases and $CuOH^{+}$ and $Cu(OH)_2$ forms can be found [45,46], which could explain the decrease in sensitivity at pH 8 and 8.5. Salinity has a significant influence only at the low salinity level (less than 25 PSU). At low salinity values, the concentration of the chloride in the artificial seawater is significantly lower and there is less chloride ions adsorbed on the surface of the electrode. Cu^{2+} ions do not need to overcome the presence of chloride ions adsorbed on the platinum to be underpotentially deposited [47]. Beyond 25 PSU, there is no significant difference between the sensitivities measured. It should also be noted that the sensitivity increases with the preconcentration times as it is expected. These results show the importance of environmental parameters (T and pH of the sea water essentially) on the Cu^{2+} detection.

3.3. Conductivity measurements

EIS experiments were run at the conductivity sensors of designs I1–I4, where real, *ReZ*, and imaginary, *ImZ*, impedance data was recorded over the frequency range 0.1 Hz–1 MHz. A range of different conductivity standard solutions was used to investigate the performance of the different sensor designs. *ReZ* was used for the conductivity measurements. The correlation between *ReZ* and the conductivity, S_{est}, is detailed in the Supplementary Data. Fig. 5 shows the conductivity values obtained experimentally using design I4 of the interdigitated electrode at 1 MHz, S_{est}, and using the conductometer readings vs. the conductivity value of the standard solutions, S_{std}. Both sensors operated similarly at the conductivity standards lower than 20.00 mS cm^{-1} with regression equations $y=0.9937x+0.0626$ for design I4 and $y=0.9119x-0.3197$ for the conductometer. Nevertheless, as opposed to the interdigitated sensor the standard conductometer readings were significantly less than the actual conductivity value in the KCl conductivity standard 50.00 mS cm^{-1}. Thus, the linearity of the conductometer over the full range of the conductivity standards deteriorated compared with the interdigitated sensor ($r^2=0.9788$ against $r^2=0.9998$ for the interdigitated sensor design I4).

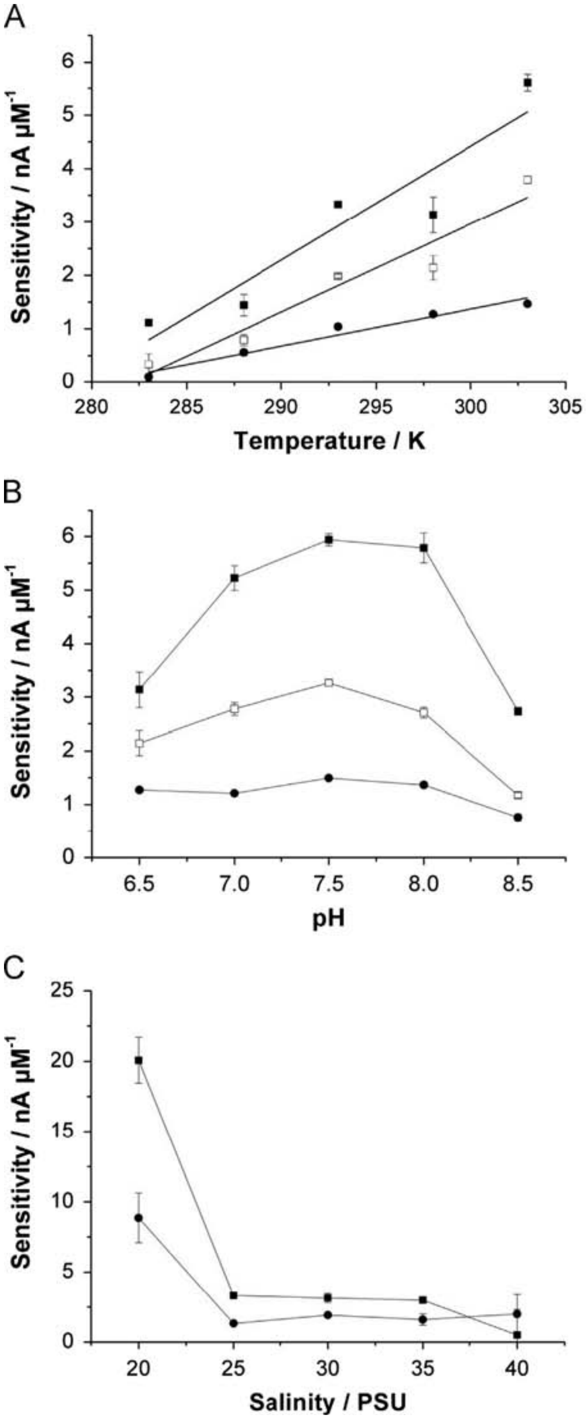

Fig. 4. Sensitivity achieved using design A6 as a function of (A) temperature (pH 6.5, 30 PSU), (B) pH ($T=298$ K, 30 PSU) and (C) salinity ($T=298$ K, pH 6.5) of the artificial seawater. Cu^{2+} concentration range was 0.5–3.0 µM for different preconcentration times: (●) PT=0 s, (□) PT=45 s and (■) PT=90 s.

4. Conclusions

Two different types of on-chip electrochemical sensors (three-electrode electrochemical cell and interdigitated electrodes) were studied with a view to using them for in-situ environmental monitoring.

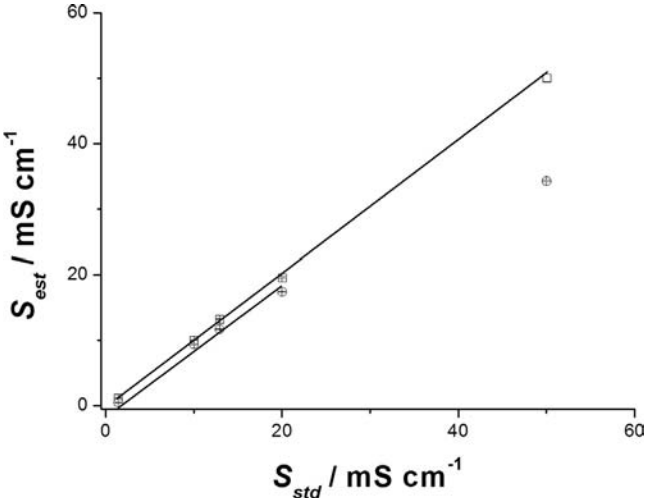

Fig. 5. Experimental conductivity measured using (○) interdigitated electrodes of design I4 at 1 MHz and (□) a commercial probe and conductometer at 2.4 kHz as a function of of the conductivity of KCl standard solutions. If not visible, the error bars are smaller than the symbols.

Cyclic voltammetry of a model redox probe at the eight different designs of microdiscs arrays have shown that microdiscs in the array behave as independent electrodes. This electrochemical behaviour is in agreement with the theory described in the literature. The different designs were then compared in terms of sensitivity and limits of detection for the detection of Cu^{2+} in artificial seawater by UPD-SV. These experiments have shown that the microdiscs do not behave independently during the UPD-SV experiments and that mixed diffusion profiles are achieved. These overlapping diffusion zones could be avoided by either reducing the preconcentration time of the Cu^{2+} UPD-SV, or by increasing the d/r ratio. Nevertheless, it is not always possible to reduce the preconcentration time in reason of the low levels of Cu^{2+} concentration that need to be detected. Furthermore, d/r cannot be increased indefinitely as it will result in a large surface area for the array and an increase of a parasitic capacitance of the corresponding non-active array area. Sensitivity of the sensors were measured for a variety of environmental conditions ($283\text{ K} < T < 303\text{ K}$; $6.5 < \text{pH} < 8.5$ and $20\text{ PSU} < \text{salinity} < 40\text{ PSU}$). T and pH had the strongest influence on the sensor response suggesting that for accurate in-situ measurements, the corresponding environmental sensors should be introduced into the sensing system. Their reading should be used to compensate the sensor measurement against T, pH and salinity. The dynamic range and limit of detections achieved for Cu^{2+} and conductivity were within the range of values observed in real samples of port and marina seawater. Furthermore, surface protection will help improve the sensitivity and the detection limits for more accurate and precise measurements.

Four designs of interdigitated electrodes were tested for the measurement of conductivity of seawater. Best results were obtained for measurements at high frequencies ($f > 10$ kHz).

Acknowledgements

The authors thank the European Commission for supporting this work (Project FP7-ICT-231646 "SHOAL: Search and monitoring of harmful contaminants, other pollutants and leaks in vessels in port using a swarm of robotic fishes").

Appendix A. Supporting information

Supplementary data associated with this article can be found in the online version at http://dx.doi.org/10.1016/j.talanta.2013.04.057.

References

[1] X.J. Huang, A.M. O'Mahony, R.G. Compton, Small 5 (2009) 779.
[2] E.P. Achterberg, C.M.G. van den Berg, C. Colombo, Cont. Shelf Res. 23 (2003) 611–623.
[3] C. Colombo, C.M.G. Van den Berg, A. Daniel, Anal. Chim. Acta 346 (1997) 101–111.
[4] M.-L. Tercier, J. Buffle, F. Graziottin, Electroanalysis 10 (1998) 355–363.
[5] M.-L. Tercier-Waeber, F. Confalonieri, G. Riccardi, A. Sina, S. Nöel, J. Buffle, F. Graziottin, Mar. Chem. 97 (2005) 216–235.
[6] C. Belmont, M.-L. Tercier, J. Buffle, G.C. Fiaccabrino, Anal. Chim. Acta 329 (1996) 203–214.
[7] R. Feeney, S. Kounaves, Anal. Chem. 72 (2000) 2222–2228.
[8] M. Sosna, G. Denuault, R.W. Pascal, R.D. Prien, M. Mowlem, Langmuir 6 (2008) 180–189.
[9] M. Sosna, G. Denuault, R.W. Pascal, R.D. Prien, M. Mowlem, Sensor Actuat. B 123 (2007) 344–351.
[10] J. Buffle, M.-L. Tercier-Waeber, TrAC Trends Anal. Chem. 24 (2005) 172–191.
[11] K. Malzahn, J.R. Windmiller, G. Valdés-Ramírez, M.J. Schöning, J. Wang, Analyst 136 (2011) 2912–2917.
[12] B. O'Flynn, F. Regan, A. Lawlor, J. Wallace, J. Torres, C. O'Mathuna, Meas. Sci. Technol. 21 (2010) 124004.
[13] A. Lawlor, J. Torres, B. O'Flynn, J. Wallace, F. Regan, Sensor Rev. 32 (2012) 29–38.
[14] G. Mills, G. Fones, Sensor Rev. 32 (2012) 17–28.
[15] T.S. Moore, K.M. Mullaugh, R.R. Holyoke, A.S. Madison, M. Yücel, G.W. Luther, Annu. Rev. Mar. Sci 1 (2009) 91–115.
[16] K.S. Johnson, J.A. Needoba, S.C. Riser, W.J. Showers, Chem. Rev. 107 (2007) 623–640.
[17] R.D. Prien, Mar. Chem. 107 (2007) 422–432.
[18] A. Berduque, Y.H. Lanyon, V. Beni, G. Herzog, Y.E. Watson, K. Rodgers, F. Stam, J. Alderman, D.W.M. Arrigan, Talanta 71 (2007) 1022–1030.
[19] A. Berduque, G. Herzog, Y.E. Watson, D.W.M. Arrigan, J.-C. Moutet, O. Reynes, G. Royal, E. Saint-Aman, Electroanalysis 17 (2005) 392–399.
[20] W. Moujahid, P. Eichelmann-Daly, J. Strutwolf, V.I. Ogurtsov, G. Herzog, D.W. M. Arrigan, Electroanalysis 23 (2011) 147–155.
[21] T.W. Biggs, H. D'Anna, Mar. Pollut. Bull. 64 (2012) 627–635.
[22] M. Srinivasan, G.W. Swain, Environ. Manage. 39 (2007) 423–441.
[23] G. Herzog, D.W.M. Arrigan, TrAC Trends Anal. Chem. 24 (2005) 208–217.
[24] J. Guo, E. Lindner, Anal. Chem. 81 (2009) 130–138.
[25] D. Menshykau, X.-J. Huang, N.V Rees, F.J. del Campo, F.X. Muñoz, R.G. Compton, Analyst 134 (2009) 343–348.
[26] G. Herzog, V. Beni, Anal. Chim. Acta 769 (2013) 10–21.
[27] J. McLaghlan, Can. J. Microbiol. 10 (1964) 769–782.
[28] J.C. Goldman, J.J. McCarthy, Limnol. Oceanogr. 23 (1978) 695–703.
[29] I. Hansson, Acta Chem. Scand. 27 (1973) 931–944.
[30] A.J. Bard, L.R. Faulkner, Eletrochemical Methods: Fundamentals and Applications, John Wiley and Sons, 2001, New York, USA.
[31] M. von Stackelberg, M. Pilgram, V. Toome, Z. Elektrochem. 57 (1953) 342–345.
[32] O. Ordeig, C.E. Banks, T.J. Davies, J. Del Campo, R. Mas, F.X. Muñoz, R. G. Compton, Analyst 131 (2006) 440–445.
[33] C.G. Zoski, N. Simjee, G. Street, O. Guenat, M. Koudelka-hep, Anal. Chem. 76 (2004) 62–72.
[34] A.M. O'Mahony, Heavy Metal Sensors for Remediation of River and Sea Water, University College Cork, Cork, Ireland, 2007.
[35] A.E. Marcinkowsky, H.O. Phillips, J. Chem. Soc. A (1971) 101–103.
[36] H.J. Lee, C. Beriet, R. Ferrigno, H.H. Girault, J. Electroanal. Chem. 502 (2001) 138–145.
[37] R. Caulcutt, R. Boddy, Statistics for Analytical Chemists, Chapman and Hall, London, United Kingdom, 1983.
[38] N. Markovic, P.N. Ross, Langmuir 9 (1993) 580–590.
[39] G. Herzog, D.W.M. Arrigan, Anal. Chem. 75 (2003) 319–323.
[40] G. Herzog, D.W.M. Arrigan, Electroanalysis 15 (2003) 1302–1306.
[41] G. Herzog, V. Beni, P.H. Dillon, T. Barry, D.W.M. Arrigan, Anal. Chim. Acta 511 (2004) 137–143.
[42] C. Belmont-Hébert, M.-L. Tercier-Waeber, J. Buffle, G.C. Fiaccabrino, N.F. De Rooij, M. Koudelka-Hep, Anal. Chem. 70 (1998) 2949–2956.
[43] L.D. Talley, in: M.C. MacCracken, J.S. Perry (Eds.), Encyclopedia of Global Environmental Change, John Wiley and Sons, Chichester, 2002, pp. 629–640.
[44] G. Jerkiewicz, F. Perreault, Z. Radovic-Hrapovic, J. Phys. Chem. C 113 (2009) 12309–12316.
[45] C.F. Baes Jr., R.E. Mesmer, Hydrolysis of Cations, John Wiley and Sons, New York, 1976.
[46] A.J. Paulson, D.R. Kester, J. Solution Chem. 9 (1980) 269–277.
[47] H.S. Yee, H.D. Abruña, Langmuir (1993) 2460–2469.